



Published in final edited form as:

AIDS. 2017 August 24; 31(13): 1819–1824. doi:10.1097/QAD.0000000000001576.

## Early initiation of antiretroviral treatment post SIV infection does not resolve lymphoid tissue activation

Jung Joo Hong<sup>1</sup>, Eduardo L V Silveira<sup>3</sup>, Praveen K Amancha<sup>2</sup>, Siddappa N Byrareddy<sup>4</sup>, Sanjeev Gumber<sup>5,6</sup>, Kyu-Tae Chang<sup>1</sup>, Aftab A Ansari<sup>5</sup>, and Francois Villinger<sup>2</sup>

<sup>1</sup>National Primate Research Center (NPRC), Korea Research Institute of Bioscience and Biotechnology (KRIBB), Cheongju, Republic of Korea

<sup>2</sup>New Iberia Research Center, University of Louisiana at Lafayette, Lafayette, LA 70560

<sup>3</sup>Department of Clinical and Toxicological Analyses, School of Pharmaceutical Sciences, University of São Paulo, São Paulo, SP 05508-000, Brazil

<sup>4</sup>Department of Pharmacology and Experimental Neuroscience, University of Nebraska Medical Center, Omaha, NE 68198

<sup>5</sup>Department of Pathology & Laboratory Medicine, Emory University School of Medicine, Atlanta, Georgia 30322, USA

<sup>6</sup>Division of Pathology, Yerkes National Primate Research Center, Emory University, Atlanta, Georgia 30329, USA

### Abstract

**Objective**—Germinal center (GC) resident follicular helper T (TFH) cells in lymphoid follicles are a potential sanctuary for HIV/SIV replication. But the dynamics of GCs upon early initiation of antiretroviral therapy (ART) and their potential role in the formation of viral sanctuaries post SIV infection are not fully understood.

**Design**—Sequential lymph node biopsies (n=10) were collected from SIVmac239-infected rhesus macaques before infection, at 5 weeks post infection/pre ART, 6 and 12 weeks following ART initiation. These tissues and cells were analyzed for frequencies of TFH cells and assignment of GC scores.

**Results**—Modest but significant increases in TFH cells and hyperplastic follicles with large GCs were noted during the acute phase of SIV infection (wk 5/pre ART). However, 6 weeks after ART initiation, substantial increases in GC TFH cells, GC B cells, hyperplastic follicles with large GCs and abundant local IL-21 production were observed, while levels of SIV RNA and DNA of lymph nodes had decreased to barely detectable values along with barely detectable levels of SIV

\*Corresponding Author. Francois Villinger, New Iberia Research Center, 4401 W Admiral Doyle Drive, New Iberia, LA 70560, Ph. 337 482 0225, Fax: 337 373 0075.

#### Author contributions

Jung Joo Hong was responsible for the concept and design of the study, performing experiments analyzing the data and writing the manuscript. Praveen K Amancha, Siddappa N Byrareddy, Eduardo L Silveira, and Sanjeev Gumber performed experiments and analyzed the data. Aftab A Ansari and Kyu-Tae Chang provided scientific input and assisted in manuscript revision. Francois Villinger was responsible for the concept and design of the study and in revising the manuscript.

antibody producing cells. An additional 6 weeks of ART did not appreciably decrease GC TFH or GC scores.

**Conclusion**—Thus, while early ART rapidly controls SIV replication, it does not regulate early lymphoid activation, which may contribute to the seeding and magnitude of viral reservoirs.

### Keywords

TFH cell; germinal center; anti-retroviral drugs

---

## Introduction

With the advent of an increasing array of anti-retroviral drugs, the outcome of clinical HIV infection has drastically improved, whereby HIV replication can be controlled to undetectable levels, virtually eliminating the development of classical AIDS [1]. However, even improved ART has so far failed to clear the infection, requiring lifelong treatment, due to the presence of long lived cellular viral reservoirs and anatomical sanctuaries even after prolonged potent viral suppression [2].

One such reservoir within lymphoid tissues are germinal center (GC) TFH cells potentially due to the physiological exclusion of CD8 T cell effectors from GC [3–5]. In the context of chronic HIV/SIV infection, a marked expansion of TFH cells has been observed in lymph nodes of patients or monkeys, compared with levels recorded at baseline or from uninfected individuals [4, 6, 7]. Although prolonged ART has been shown to decrease the relative frequency of GC TFH cells in lymph nodes, their representation still remains significantly elevated relative to healthy individuals [6, 7]. However, the dynamic of GC TFH cells during early ART initiation has not been well documented, which has implications in the seeding and maintenance of viral reservoirs [8]. In efforts to evaluate whether inhibition of SIV replication would inhibit lymphoid hyperplasia, we investigated the dynamics of lymphoid activation longitudinally during early chronic infection, with ART initiated before the appearance of full blown follicular hyperplasia post SIV infection [9].

## Materials and Methods

All animals used in this study were born and maintained at the Yerkes National Primate Research Center of Emory University in accordance with the regulations of the Guide on the Care and Use of Laboratory Animal Resources. All experiments were approved by the Emory Institutional Animal Care and Use and Biosafety Committees. The animals were inoculated with 200 TCID<sub>50</sub> (50% tissue culture infectious doses) of SIVmac239 intravenously and served as a source for blood and lymph node biopsies at various time points post infection.

### ART treatment

ART comprised a 3 drug regimen including: 9-R-(2-phosphonomethoxypropyl) adenine (PMPA, 20mg/kg/day) and Emtricitabine (FTC, 30 mg/kg/day) both from Gilead and administered subcutaneously and an integrase inhibitor (Raltegravir, 100 mg per day orally, courtesy of Merck) initiated at 5 weeks post SIV infection for 3 months.

**Quantitation of SIV RNA/DNA in Plasma and lymph nodes**—Plasma SIV RNA load and cellular SIV DNA/RNA were determined by quantitative RT-PCR and PCR as described previously [10].

### Flow cytometry

Peripheral lymph nodes were collected at baseline before SIV infection, and at 5, 11 and 17 weeks post infection (wpi) and processed for in situ analyses as well as for isolating mononuclear cells as previously described [11, 12]. One million freshly isolated mononuclear cells were stained for live/Dead marker (Alexa 430 Invitrogen A10169) and then stained with predetermined concentrations of antibodies against CD3 (SP34-2), CD4 (L200), CD8 (RPA-T8), CD20 (L27), CD28 (CD28.2), CD95 (DX2) and PD1 (EH12.2H7). Cells were incubated with the antibody cocktail for 30 min at 4°C, washed with PBS containing 2% Fetal Bovine Serum, cells were then fixed in 1% paraformaldehyde (PFA), and the data acquired on LSR-II flow cytometer driven by FACS DiVa software. Analysis of the acquired data was performed using FlowJo software (version 9.2; TreeStar, Ashland, OR).

### Immunofluorescent staining and quantitative image analysis

Staining procedures were performed as described previously [9, 13]. Lymph node sections were cut (4 to 5 µm) and incubated with mouse anti-human Ki67 (Vector), rabbit anti-human CD20 (Thermo scientific), and goat anti-human PD1 (R&D system) antibodies after heat-induced epitope retrieval. Sections were also stained for SIVgag p17 using mouse anti-p27 (KK59, NIH AIDS Repository Reagent Program). Thereafter, the sections were counter-stained with Hoechst 33342 (Invitrogen). Every step was followed by three washes with TBS automation buffer (Biocare). All images were acquired with an Axio Imager Z1 microscope (Zeiss) using various objectives. The GC size was calculated based on both nucleus dye and Ki67 staining of GC B cells in AxioVs40 V4.8.1.0 program (Zeiss), as described previously [9]. The hematoxylin and eosin stained lymph node sections were blindly evaluated by a veterinary pathologist.

### ELISPOT

Standard ELISPOT assays were performed as described previously [14]. Ninety six well plates (EMD Millipore, Billerica, MA, USA) were coated with 10 µg/mL of anti-monkey IgG, IgA and IgM (H&L) goat antibody (Rockland Immunochemicals, Pottstown, PA, USA) or 2 µg/mL of recombinant SIV ENV overnight at 4 °C for enumeration of antibody secreting cells (ASCs). Wells were blocked with complete RPMI medium for 2 h at 37 °C. Whole lymph node cell preparations were diluted, plated in serial 3-fold dilutions and incubated overnight at 37 °C. Wells were then incubated for 2h at RT with biotin-conjugated anti-monkey IgG (Rockland), diluted 1:1000 in PBS with 0.05% Tween 20 and 1% FBS. Wells were incubated for 3h at RT with Avidin D-HRP (Vector labs, Burlingame, CA, USA), diluted 1:1000. Spots were developed with filtered 3-amino-9-ethylcarbazole substrate and then counted using the Immunospot CTL counter and the Image Acquisition v4.5 software (Cellular Technology, Shaker Heights, OH, USA).

## Results

Ten rhesus macaques (RMs) were injected with SIVmas239 intravenously, allowed to undergo acute infection and initiated on daily ART at 5 wpi for 3 months. Plasma SIV RNA levels reached their peak replication at about 2 wpi and early viral load set points by 5 wpi ( $10^4$ – $10^6$  vRNA copies/ml). By 7 wpi (2 weeks after ART initiation), 9 out of 10 monkeys had plasma viral loads below the detection limit of the assay (50 copies/ml) while the last animal reached that level at 8 wpi (Figure 1D). In lymph nodes, quantification of SIV RNA and DNA showed a significant decrease in the level of both replicating virus RNA and proviral DNA in lymph node cells collected from 5 to 11 wpi and a second order decrease from 11 and 17 wpi under ART (Figure 1E).

GC TFH cells were defined by high density PD-1 expression of gated central memory CD4 T cells as previously described (Figure 1A). The frequency of GC TFH cells was monitored at baseline, 5, 11 and 17 wpi (Figure 1B). Although the kinetics of early expansion of TFH showed considerable individual differences as previously reported [9], by 5 wpi, a significant, albeit modest, overall increase in TFH frequencies was noted ( $8.3 \pm 1.4\%$ ,  $p=0.0095$ ). We had previously demonstrated a marked TFH expansion by 4 months post infection in the absence of ART [9]. Surprisingly, in spite of the profound control of viral replication induced by ART to almost undetectable levels, a marked expansion of TFH cells was noted in all animals on ART from 5 to 11 wpi ( $19.7 \pm 2.7\%$  at 11 wpi). These increased levels were maintained at 17 wpi ( $16.31 \pm 3.3\%$ ), suggesting that lymphoid activation was not directly linked to levels of viral replication *in vivo*. At that stage of infection, TFH expansion in ART treated monkeys was lower than in monkeys infected with the same stock and route of SIVmac239 without ART treatment ( $16.31 \pm 3.3\%$  at 17 wpi for ART treated vs  $48.2 \pm 5.3\%$  at 16–19 wpi for untreated monkeys) [9].

The functional consequence of TFH and GC expansion was tested by enumerating the number of total IgG and SIV Env (gp140)-specific IgG secreting cells (ASC) pre and during ART. Relatively high frequencies of SIV Env-specific ASCs were detected at 5 wpi in lymph nodes that markedly decreased after 6 weeks of ART (Supplemental figure 1B,  $1131.9 \pm 188.7\%$  at 4 wpi, and  $225.8 \pm 57.7\%$  at 11 wpi,  $P=0.0008$ ), suggesting that differentiation of antigen specific and overall B cells into ASCs is indeed linked to the magnitude of virus replication.

Increases in TFH cells are generally associated with histological changes of the lymphoid architecture, in particular, a more delineated definition of the follicles and formation of GCs. We next investigated the sequential development of GCs in lymph nodes from the same RMs using *in situ* methods as previously described [4, 9]. Consistent with the increased frequencies of TFH cells measured by flow cytometry (Figure 1), the relative GC size was significantly increased at 5 wpi compared to baseline ( $9.7 \pm 2.9\%$  at 0 wpi vs  $22.9 \pm 4.0\%$  at 4 wpi,  $p=0.0095$ ) (Figure 2). The increase in activated B cells was confirmed by Flow cytometry in this compartment and these cells were shown to be present primarily in the GC (Supplemental figure 2). However, this expansion was not uniform across all animals with a direct correlation with relative GC size and TFH frequencies (data not shown). At 11 wpi, the relative GC size had increased to  $54.3 \pm 5.0\%$ , with non-significant decrease to 39.6

± 4.3% by 17 wpi (12 weeks on ART). Similar to observations made during chronic untreated SIV infection [4, 9], the accumulation of proliferating B cells was restricted to GCs of hyperplastic follicles, associated and potentially resulting from the high expression of IL-21 (Figure 2A and B). By contrast, few SIV Gag P17 stained cells were detected in hyperplastic follicles after 3 months of ART (Figure 2B). Of interest, the relative size of GCs within B cell follicles developed to a rate similar to the one observed in hyperplastic follicles from lymph nodes of typical untreated SIV progressors by 16~19 wpi ( $54.4 \pm 3.5\%$  at 16~19wpi) [9], suggesting that the development of follicular hyperplasia is associated with local production of IL-21 rather than levels of virus present within GCs.

## Discussion

TFH cells are central to the formation and development of GCs and elicitation of a durable humoral response in lymphoid tissues [15] upon antigen specific stimulation, via either immunization or in response to infection [16, 17]. During the course of HIV/SIV infections, lymphadenopathy is a hallmark of inflammation, including an accumulation of a heterogeneous array of GC TFH cell subsets in lymphoid follicles [4, 18–20]. Since GC TFH cells are also targets of HIV/SIV infection [19, 21, 22], the extensive expansion of this compartment and its maintenance during infection needs to be taken into consideration when addressing viral reservoirs during ART.

In the SIV infected macaque model, significant changes in the lymphoid architecture and expansion of TFH in lymph nodes occur at the early chronic infection stage compared with uninfected and acutely infected RMs [4, 23]. It was hypothesized that early elimination of viremia prior to fully developed lymphoid hyperplasia would result in a return to baseline values for GC size and TFH frequencies, given the potent control of viral replication by ART *in vivo*. Quite surprisingly, our results show unequivocally that the follicular hyperplasia initiated by the acute infection developed at about the same rate and almost to the same magnitude as the ones observed in SIV infected but untreated monkeys [23]. This maintenance of expansion was not fueled by SIV antigen as demonstrated by decreased viral loads in the local tissue as well as ASCs under ART (supplemental fig1B) [24, 25], but appears associated with elevated levels of cytokines such as IL-21, that resulted from the initial acute infection [26]. This protracted activation of lymphoid tissues long beyond elimination of active viral replication *in vivo* suggests that the resolution of this immune activated state likely will require extensive time on ART to decrease back to “normal levels”, if ever. The maintenance of GC TFH cells has traditionally thought to be due to several factors, including 1) a relatively lower concentration of anti-HIV drugs within the lymphoid compartment relative to blood, allowing for the continued low level replication in these tissues (a.k.a. smoldering infection) [27], 2) a GC niche with follicular dendritic cells which may contain viral proteins such as p24 antigen that persist longer without virus replication under ART [28, 29], 3) low levels of replicating virus from activated GC TFH cells, which might suffice to recruit new cells to GCs and maintain the cycle [5] and 4) residual HIV-immune reconstitution inflammatory syndrome (IRIS), encompassing pro-inflammatory IL-6, TNF- $\alpha$  and others, that may play a paramount role in maintaining TFH cells and GC responses in RMs receiving ART [30]. While there is data in support of each mechanism cited, an important observation has been the fact that GC TFH cells were recently shown to

represent a critical reservoir and even maintain persistent productive virus infection, compared with non-TFH cells in SIV infected elite controller macaques [5] and human patients on ART [31]. Our present data suggest that follicular hyperplasia is ongoing irrespective of the continued presence of viral antigen, and this hyperplasia provides a viral reservoir from which virus has been shown to rebound upon ART cessation [32, 33]. Thus, an intact GC environment with accumulation of TFH cells in hyperplastic follicles acts as the crucial niche from which virus replication can rapidly rekindle upon ART interruption. While our data do not definitely identify the mechanism at play during ART, we submit that the demonstration of continued lymphoid hyperplasia in the absence of extensive viral replication may represent another issue that should be considered therapeutically. For these reasons, we suggest that manipulation of GC architecture in lymphoid follicles might provide a testable therapeutic approach to attempt to control virus rebound after ART cessation. Of note, transplantation studies are underway to test which combination of immunosuppressive drugs attenuate GC-related donor-specific antibody production in experimental transplantation [13, 34, 35]. Indeed, blockade of CD28-mediated signals significantly altered GC formation in a monkey renal transplant model [13], which could represent yet another avenue to contain the viral reservoir in its latent state.

## Supplementary Material

Refer to Web version on PubMed Central for supplementary material.

## Acknowledgments

The authors would like to thank the staff and veterinarians of the Yerkes National Primate Research Center for their excellent care of the animals, Dr. Gelezunias (Gilead) for the gift of PMPA and FTC, Dr. Hazuda (Merck) for the provision of integrase inhibitor and the NIH ARRRP for the provision of the KK59 Mab.

This work was supported in part by NIH grants R01 AI078775 and 8R24OD010947 to F Villinger, NIH grant R01 AI098628 to AA Ansari, NIH OD-51OD11132 to the Yerkes NPRC.

## References

1. Piot P, Quinn TC. Response to the AIDS pandemic--a global health model. *N Engl J Med.* 2013; 368:2210–2218. [PubMed: 23738546]
2. Shehu-Xhilaga M, Tachedjian G, Crowe SM, Kedzierska K. Antiretroviral compounds: mechanisms underlying failure of HAART to eradicate HIV-1. *Curr Med Chem.* 2005; 12:1705–1719. [PubMed: 16029143]
3. Connick E, Mattila T, Folkvord JM, Schlichtemeier R, Meditz AL, Ray MG, et al. CTL fail to accumulate at sites of HIV-1 replication in lymphoid tissue. *J Immunol.* 2007; 178:6975–6983. [PubMed: 17513747]
4. Hong JJ, Amancha PK, Rogers K, Ansari AA, Villinger F. Spatial alterations between CD4(+) T follicular helper, B, and CD8(+) T cells during simian immunodeficiency virus infection: T/B cell homeostasis, activation, and potential mechanism for viral escape. *J Immunol.* 2012; 188:3247–3256. [PubMed: 22387550]
5. Fukazawa Y, Lum R, Okoye AA, Park H, Matsuda K, Bae JY, et al. B cell follicle sanctuary permits persistent productive simian immunodeficiency virus infection in elite controllers. *Nat Med.* 2015
6. Perreau M, Savoye AL, De Crignis E, Corpataux JM, Cubas R, Haddad EK, et al. Follicular helper T cells serve as the major CD4 T cell compartment for HIV-1 infection, replication, and production. *J Exp Med.* 2013; 210:143–156. [PubMed: 23254284]

7. Lindqvist M, van Lunzen J, Soghoian DZ, Kuhl BD, Ranasinghe S, Kranias G, et al. Expansion of HIV-specific T follicular helper cells in chronic HIV infection. *J Clin Invest.* 2012; 122:3271–3280. [PubMed: 22922259]
8. Whitney JB, Hill AL, Sanisetty S, Penaloza-MacMaster P, Liu J, Shetty M, et al. Rapid seeding of the viral reservoir prior to SIV viraemia in rhesus monkeys. *Nature.* 2014; 512:74–77. [PubMed: 25042999]
9. Hong JJ, Amancha PK, Rogers KA, Courtney CL, Havenar-Daughton C, Crotty S, et al. Early lymphoid responses and germinal center formation correlate with lower viral load set points and better prognosis of simian immunodeficiency virus infection. *J Immunol.* 2014; 193:797–806. [PubMed: 24907346]
10. Byrareddy SN, Kallam B, Arthos J, Cicala C, Nawaz F, Hiatt J, et al. Targeting alpha4beta7 integrin reduces mucosal transmission of simian immunodeficiency virus and protects gut-associated lymphoid tissue from infection. *Nat Med.* 2014; 20:1397–1400. [PubMed: 25419708]
11. Amancha PK, Hong JJ, Rogers K, Ansari AA, Villinger F. In Vivo Blockade of the Programmed Cell Death-1 Pathway Using Soluble Recombinant PD-1-Fc Enhances CD4+ and CD8+ T Cell Responses but Has Limited Clinical Benefit. *J Immunol.* 2013; 191:6060–6070. [PubMed: 24227774]
12. Hong JJ, Amancha PK, Rogers K, Ansari AA, Villinger F. Re-evaluation of PD-1 expression by T cells as a marker for immune exhaustion during SIV infection. *PLoS One.* 2013; 8:e60186. [PubMed: 23555918]
13. Kim EJ, Kwun J, Gibby AC, Hong JJ, Farris AB 3rd, Iwakoshi NN, et al. Costimulation blockade alters germinal center responses and prevents antibody-mediated rejection. *Am J Transplant.* 2014; 14:59–69. [PubMed: 24354871]
14. Silveira EL, Kasturi SP, Kovalenkova Y, Rasheed AU, Yeiser P, Jinnah ZS, et al. Vaccine-induced plasmablast responses in rhesus macaques: phenotypic characterization and a source for generating antigen-specific monoclonal antibodies. *J Immunol Methods.* 2015; 416:69–83. [PubMed: 25445326]
15. Crotty S. T follicular helper cell differentiation, function, and roles in disease. *Immunity.* 2014; 41:529–542. [PubMed: 25367570]
16. Hong JJ, Chang KT, Villinger F. The Dynamics of T and B Cells in Lymph Node during Chronic HIV Infection: TFH and HIV, Unhappy Dance Partners? *Front Immunol.* 2016; 22 <http://dx.doi.org/10.3389/fimmu.2016.00522>.
17. Crotty S. T follicular helper cell differentiation, function, and roles in disease. *Immunity.* 2014; 41:529–542. [PubMed: 25367570]
18. Petrovas C, Yamamoto T, Gerner MY, Boswell KL, Wloka K, Smith EC, et al. CD4 T follicular helper cell dynamics during SIV infection. *J Clin Invest.* 2012; 122:3281–3294. [PubMed: 22922258]
19. Velu V, Mylvaganam GH, Gangadhara S, Hong JJ, Iyer SS, Gumber S, et al. Induction of Th1-Biased T Follicular Helper (Tfh) Cells in Lymphoid Tissues during Chronic Simian Immunodeficiency Virus Infection Defines Functionally Distinct Germinal Center Tfh Cells. *J Immunol.* 2016; 197:1832–1842. [PubMed: 27481845]
20. Ueno H. Human Circulating T Follicular Helper Cell Subsets in Health and Disease. *J Clin Immunol.* 2016
21. Mylvaganam GH, Velu V, Hong JJ, Sadagopal S, Kwa S, Basu R, et al. Diminished viral control during simian immunodeficiency virus infection is associated with aberrant PD-1hi CD4 T cell enrichment in the lymphoid follicles of the rectal mucosa. *J Immunol.* 2014; 193:4527–4536. [PubMed: 25246494]
22. Hufert FT, van Lunzen J, Janossy G, Bertram S, Schmitz J, Haller O, et al. Germinal centre CD4+ T cells are an important site of HIV replication in vivo. *AIDS.* 1997; 11:849–857. [PubMed: 9189209]
23. Hong JJ, Amancha PK, Rogers KA, Courtney CL, Havenar-Daughton C, Crotty S, et al. Early lymphoid responses and germinal center formation correlate with lower viral load set points and better prognosis of simian immunodeficiency virus infection. *J Immunol.* 2014; 193:797–806. [PubMed: 24907346]

24. Notermans DW, de Jong JJ, Goudsmit J, Bakker M, Roos MT, Nijholt L, et al. Potent antiretroviral therapy initiates normalization of hypergammaglobulinemia and a decline in HIV type 1-specific antibody responses. *AIDS Res Hum Retroviruses*. 2001; 17:1003–1008. [PubMed: 11485617]
25. Kalams SA, Goulder PJ, Shea AK, Jones NG, Trocha AK, Ogg GS, et al. Levels of human immunodeficiency virus type 1-specific cytotoxic T-lymphocyte effector and memory responses decline after suppression of viremia with highly active antiretroviral therapy. *J Virol*. 1999; 73:6721–6728. [PubMed: 10400770]
26. Katsikis PD, Mueller YM, Villinger F. The cytokine network of acute HIV infection: a promising target for vaccines and therapy to reduce viral set-point? *PLoS Pathog*. 2011; 7:e1002055. [PubMed: 21852945]
27. Fletcher CV, Staskus K, Wietgreffe SW, Rothenberger M, Reilly C, Chipman JG, et al. Persistent HIV-1 replication is associated with lower antiretroviral drug concentrations in lymphatic tissues. *Proc Natl Acad Sci U S A*. 2014; 111:2307–2312. [PubMed: 24469825]
28. Orenstein JM, Feinberg M, Yoder C, Schragger L, Mican JM, Schwartzentruber DJ, et al. Lymph node architecture preceding and following 6 months of potent antiviral therapy: follicular hyperplasia persists in parallel with p24 antigen restoration after involution and CD4 cell depletion in an AIDS patient. *AIDS*. 1999; 13:2219–2229. [PubMed: 10563707]
29. Tenner-Racz K, Stellbrink HJ, van Lunzen J, Schneider C, Jacobs JP, Raschdorff B, et al. The unenlarged lymph nodes of HIV-1-infected, asymptomatic patients with high CD4 T cell counts are sites for virus replication and CD4 T cell proliferation. The impact of highly active antiretroviral therapy. *J Exp Med*. 1998; 187:949–959. [PubMed: 9500797]
30. Bonham S, Meya DB, Bohjanen PR, Boulware DR. Biomarkers of HIV Immune Reconstitution Inflammatory Syndrome. *Biomark Med*. 2008; 2:349–361. [PubMed: 19057654]
31. Banga R, Procopio FA, Noto A, Pollakis G, Cavassini M, Ohmiti K, et al. PD-1(+) and follicular helper T cells are responsible for persistent HIV-1 transcription in treated aviremic individuals. *Nat Med*. 2016; 22:754–761. [PubMed: 27239760]
32. Horiike M, Iwami S, Kodama M, Sato A, Watanabe Y, Yasui M, et al. Lymph nodes harbor viral reservoirs that cause rebound of plasma viremia in SIV-infected macaques upon cessation of combined antiretroviral therapy. *Virology*. 2012; 423:107–118. [PubMed: 22196013]
33. Rothenberger MK, Keele BF, Wietgreffe SW, Fletcher CV, Beilman GJ, Chipman JG, et al. Large number of rebounding/founder HIV variants emerge from multifocal infection in lymphatic tissues after treatment interruption. *Proc Natl Acad Sci U S A*. 2015; 112:E1126–34. [PubMed: 25713386]
34. Burghuber CK, Kwun J, Page EJ, Manook M, Gibby AC, Leopardi FV, et al. Antibody-Mediated Rejection in Sensitized Nonhuman Primates: Modeling Human Biology. *Am J Transplant*. 2016; 16:1726–1738. [PubMed: 26705099]
35. Kwun J, Page E, Hong JJ, Gibby A, Yoon J, Farris AB, et al. Neutralizing BAFF/APRIL with atacicept prevents early DSA formation and AMR development in T cell depletion induced nonhuman primate AMR model. *Am J Transplant*. 2015; 15:815–822. [PubMed: 25675879]

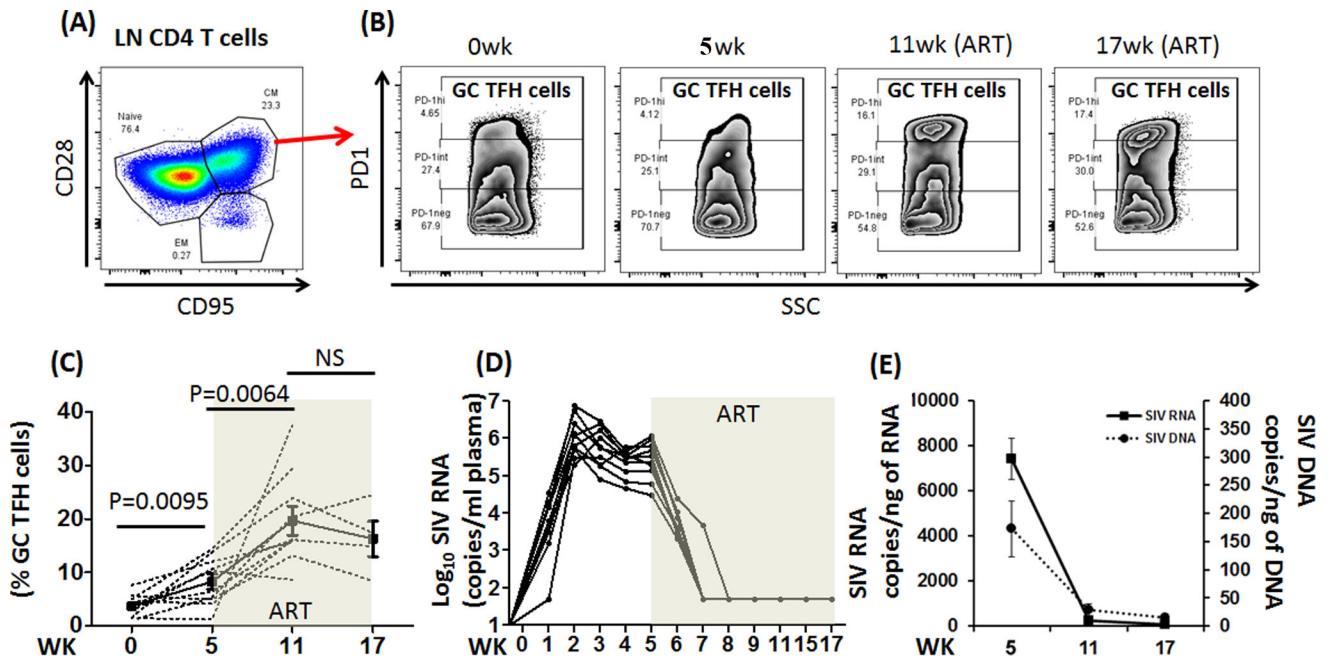


**Figure 1.**

Dynamics of GC TFH cells in lymph nodes before and during ART in SIV infection (A) Gating strategy utilized for the identification of GC TFH cells, (live single cells/CD20<sup>-</sup>/CD3<sup>+</sup>/CD8<sup>-</sup>/CD4<sup>+</sup>/CD28<sup>+</sup>/CD95<sup>+</sup>/PD-1<sup>hi</sup>). (B) Representative frequencies of GC TFH cells prior to SIV infection (0 wk) and during early SIV infection before ART (4 wk). ART was initiated at week 5 and samples obtained at 6 weeks and 12 weeks post ART initiation (11 wk and 17 wk, respectively post SIV infection). (C) Percentage of GC TFH cells in lymph nodes. Samples were collected longitudinally from 10 rhesus macaques at week 0, 5, and 11 post-infection, and 4 animals at week 17 post-infection. Values from each individual monkey (dotted line) are shown as well as the means with standard errors (solid line). (D) Plasma SIV RNAs dynamics before and during ART. (E) Lymph node SIV RNA and DNA load from three macaques from each time point

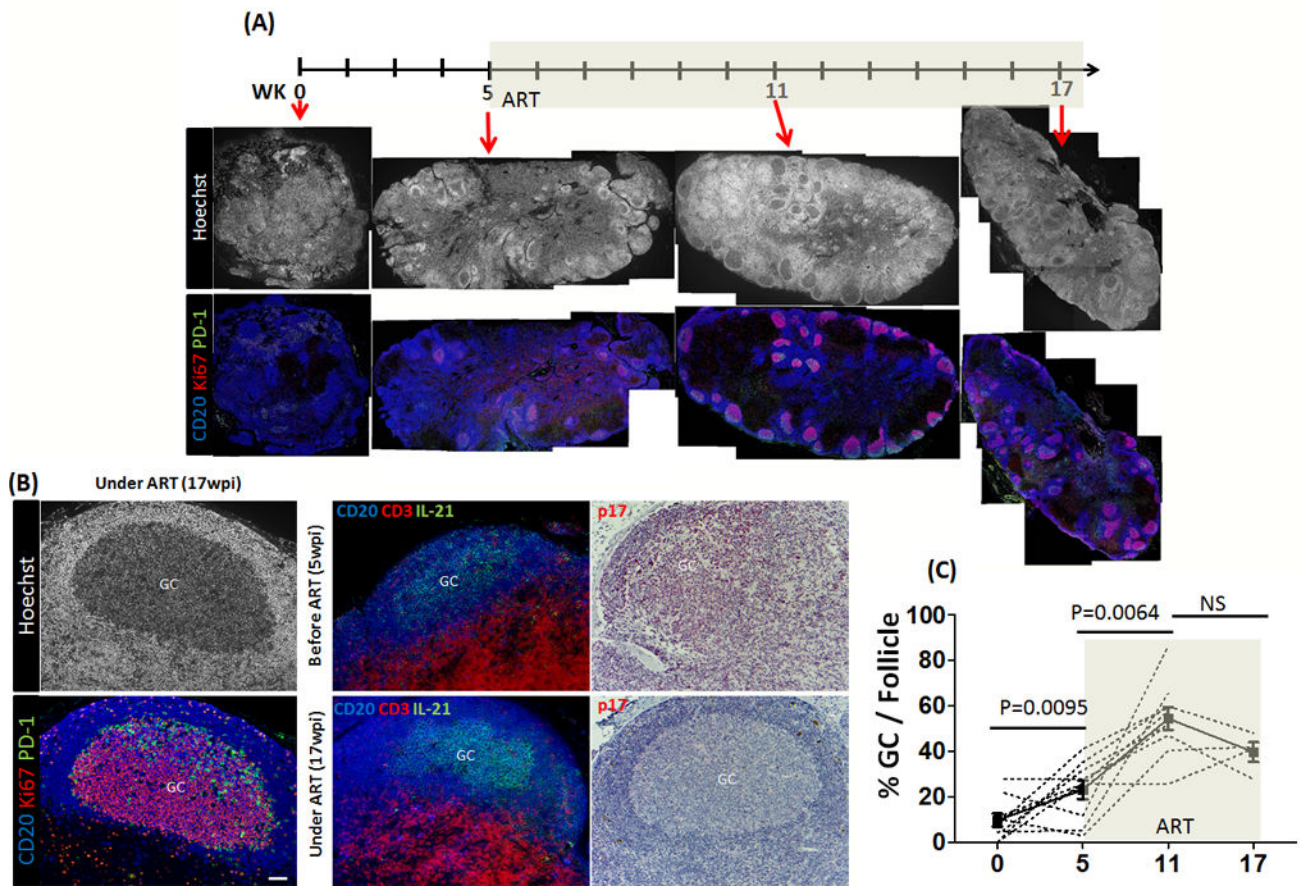


**Figure 2.**

Dynamics of GCs in lymph nodes before and during ART in SIV infection (A) The longitudinal development of hyperplastic follicles with large GCs is illustrated in whole sections of peripheral lymph nodes biopsied from the same animal (RBe14) at 0, 5, 11, and 17 wpi. The top panels illustrate the patterns seen with Hoechst staining and the bottom panels illustrate the staining observed following staining with CD20 (blue), Ki-67 (red) and PD-1 (green). (B) Representative enlarged images of the structure of a hyperplastic follicle (Left panels) under ART. Representative IL-21 expression (Middle panels) and SIV gag p17 staining (Right panels) were shown for the hyperplastic follicles before and under ART. (C) Evolution of the GC size relative to the follicle area in lymph nodes collected longitudinally from 10 RMs at 0, 5, and 11 wpi and 4 RMs at 17 wpi. Each dotted line represents sequential samples from individual monkeys and the mean (solid line) is represented with standard error.